Rare Metal Materials and Engineering
Volume 49, Issue 9, September 2020
Available online at www.rmme.ac.cn

Science Press

Cite this article as: Rare Metal Materials and Engineering, 2020, 49(9): 3005-3011.

ARTICLE

Microstructural Evolution of Ti-6Al-4V Alloy During Water Quenching Under Different Processing Conditions

Zhang Runqi[1], Cai Yiqin[1], Li Zhuang[1], Li Jinyu[1], Zhou Qi[2], Cui Xijun[1]

[1] College of Materials Science and Engineering, Shenyang Aerospace University, Shenyang 110136, China; [2] School of Environment and Chemical Engineering, Shenyang Ligong University, Shenyang 110159, China

Abstract: It is important to understand the microstructural evolution of Ti-6Al-4V alloy during water quenching under different processing parameters in order to obtain optimum mechanical properties of the alloy. The thermal simulation of Ti-6Al-4V alloy was conducted using a thermomechanical simulator. The results have shown that a fully martensitic microstructure was obtained after solution treatment. Water-quenching after solution resulted in hardness increase, and this was attributed to the presence of α' and α''. The lamellar structure formed when the specimen was water-quenched after isothermal holding at 850 °C, and the hardness further increased. Colony appeared after deformation at 850 °C with subsequent water quenching, and the Vickers hardness HV reached the maximum value (5840 MPa) because of the grain boundary strengthening. The microstructure was composed of α phase, lamellar colonies α/β and colony when the specimen was isothermally held at 600 °C after deformation at 850 °C. Cooling and isothermal holding after deformation increased the width of α phase and colony, which was in the range of 324~706 nm for equiaxed grains. This caused a decrease in hardness.

Key words: Ti-6Al-4V alloy; water quenching; isothermal holding; the lamellar structure; hardness

Titanium alloys are widely used due in many fields to their high specific strength, fatigue resistance, corrosion resistance and biocompatibility[1-4]. $\alpha+\beta$ alloys have the composition that supports a mixture of α and β phases and may contain β phase between 10% and 50% at room temperature. The most common $\alpha+\beta$ alloy is Ti-6Al-4V, which is usually quenched by water to obtain a good balance of mechanical properties[5-9].

AS a two phase titanium alloy, Ti-6Al-4V can display a wide range of microstructures depending on the thermomechanical or thermal processing routes[10-14]. Early work on titanium alloys processing mainly focused on morphology modification of the initial $\alpha+\beta$ phase microstructure in Ti-6Al-4V alloy to convert the lamellar morphology to an equiaxed grain structure through thermomechanical processing (TMP) [7]. Zherebtsov et al. [15] have studied microstructure evolution during warm working of titanium alloy at 600 and 800 °C. The properties of titanium alloys at different temperatures as functions of processing parameters and heat treatment cycle can be predicted [16]. To understand and control the relationships of processing-structure-property, Ding et al. [17] have studied the variation of microstructure of the Ti-6A1-4V alloy during thermomechanical processing in a range of hot working conditions. It is necessary to make clear an appropriate control of processing parameters such as reheat temperature, deformation condition and isothermal processing in order to obtain optimum mechanical properties.

In general, the mechanical properties of titanium alloy are determined by its final microstructure. In this study, thermal simulations were conducted in Ti-6Al-4V alloy. The Vickers hardness distributions of the specimens were evaluated from. Great attention was paid to the effect of different processing conditions on the microstructural characteristics of Ti-6Al-4V alloy. All the analyses were based on the experimental results in the thermal simulation specimens.

1 Experiment

Cylindrical specimens with 8 mm in diameter and 15 mm

Received date: September 09, 2019
Foundation item: National High Technology Research and Development Program of China (863 Program) (2015AA03A501); Liaoning Provincial Science and Technology Plan Project (2015020189)
Corresponding author: Li Zhuang, Ph. D., Professor, College of Materials Science and Engineering, Shenyang Aerospace University, Shenyang 110136, P. R. China, Tel: 0086-24-31523380, E-mail: lizhuang20047@163.com

in height for thermal simulation tests, were cut from an as-received, commercially available Ti-6Al-4V alloy with chemical composition shown in Table 1. Thermal simulation experiments were performed in a Gleeble 1500 thermo-mechanical simulator, and the processing schedule is shown in Fig. 1; P1, P2, P3 and P4 are Processing 1, 2, 3 and 4, respectively.

Measurements of the Vickers hardness used a total of 5 indentations under a load of 500 g for each specimen of the processing conditions. The specimens for optical microscopy (OM) and scanning electron microscopy (SEM, SSX-550) observation were etched with a solution of HF (5 mL) + HNO_3 (15 mL) + H_2O (25 mL). The foils for transmission electron microscopy (TEM, EM 400T) observation were prepared by twin jet polishing using a solution of 10% perchloric acid in methanol at −30 °C and the operating voltage of 40 V. The phase composition in the specimens after thermal simulations was determined using an X-ray diffractometer (D/max2400) with Cu Kα radiation.

2 Results and Discussion

2.1 Hardness and stress-strain curve

2.1.1 Vickers hardness

The variation in Vickers hardness HV of all specimens with different processing parameters is shown in Fig.2. The lowest value of Vickers hardness (1850 MPa) was obtained for the specimen of the initial state. Direct water-quenching to room temperature after solution resulted in hardness increase, and the hardness of P1 specimen increased up to 3970 MPa. The hardness of P2 specimen further increased after isothermal holding at 850 °C. The maximum hardness (5840 MPa) of P3 specimen was obtained when the specimen was water-quenched after deformation. The hardness of P4 specimen after isothermal holding at 600 °C decreased down to 5190 MPa.

Table 1 Chemical composition of as received Ti-6Al-4V alloy (wt%)

Al	V	C	Fe	N	O	H	Ti
5.71	3.83	0.052	0.047	0.009	0.187	0.006	Bal.

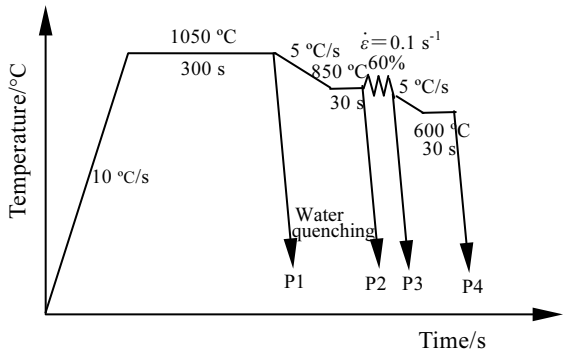

Fig.1 Schematic illustrations describing the thermal conditions of the simulation

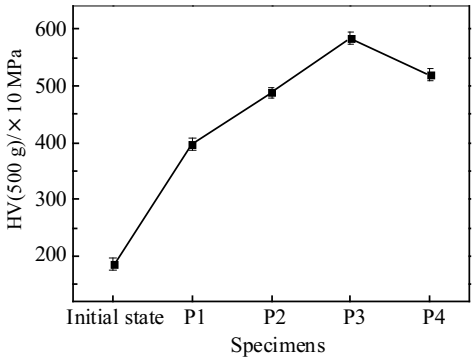

Fig.2 Vickers hardness of the specimens under different processing conditions

2.1.2 Stress-strain curve

Fig. 3 shows true stress-true strain curve of P3 specimen. The flow curve exhibited a peak point at relatively low strain, and it was followed by flow softening at larger strains.

2.2 Microstructures of the specimens

2.2.1 Optical microscopy microstructure

Initial microstructure before TMP is shown in Fig.4. The microstructure of Ti-6Al-4V alloy consisted of lamellar-α colonies and prior β grains. Primary α phase was observed.

A fully martensitic microstructure was observed in Ti-6Al-4V alloy after solution treatment. The micrographs of this specimen are indicated in Fig.5.

Optical micrographs of specimens under three processing conditions are presented in Fig. 6. The specimen which was water-quenched after isothermal holding at 850 °C showed the formation of the lamellar structure, and platelet α taken parallel to each other (Fig. 6a). Colony began to form after deformation with subsequent water quenching, and at the same time the metastable Widmanstatten structure became more stable colony (Fig.6b). The microstructure of P4

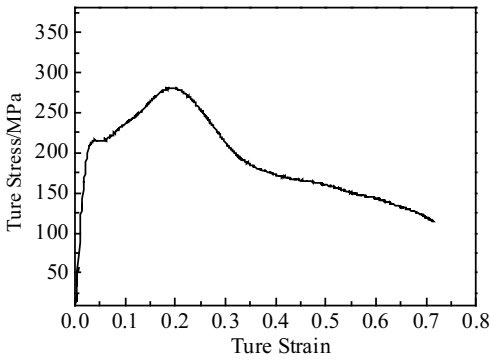

Fig.3 True stress-true strain curve of P3 specimen with isothermal compression at 850 °C at strain rate of 0.1 s^{-1}

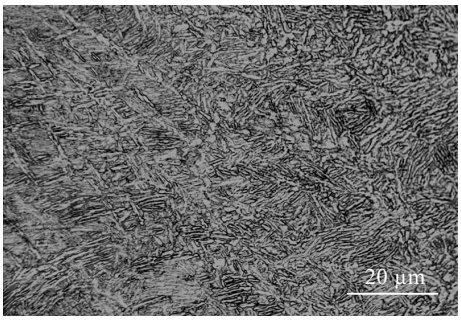

Fig.4 OM micrograph of initial specimen

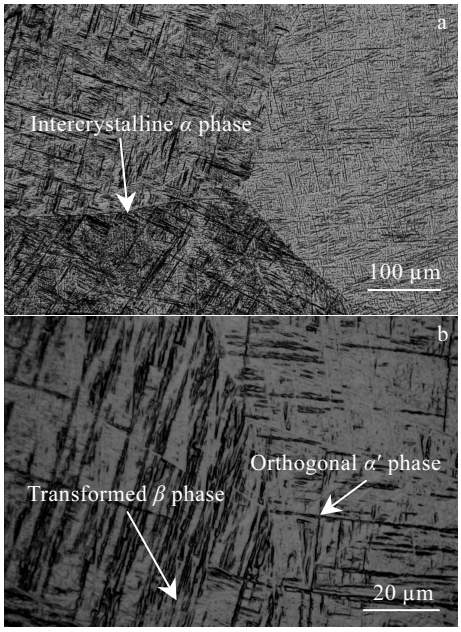

Fig.5 OM micrographs of the specimen after solution treatment: (a) intercrystalline α phase; (b) the transformed β phase and orthogonal α' plate

specimen after isothermal holding at 600 °C were composed of α phase and lamellar colonies α/β. Colony increased (Fig. 6c).

2.2.2 SEM and TEM observation

Fig.7 provides an overview of SEM micrographs of specimens under four processing conditions. P1 specimen exhibited orthogonal α' plates (Fig.7a). Coarse lamellar of α-phases were observed, and the width of Widmanstatten α-phase reached 4 μm for P2 specimen (Fig.7b). α plates became very fine due to the deformation except for the colony in P3 specimen (Fig.7c). The width of α phase increased and colony existed within the lamellar structure (Fig.7d).

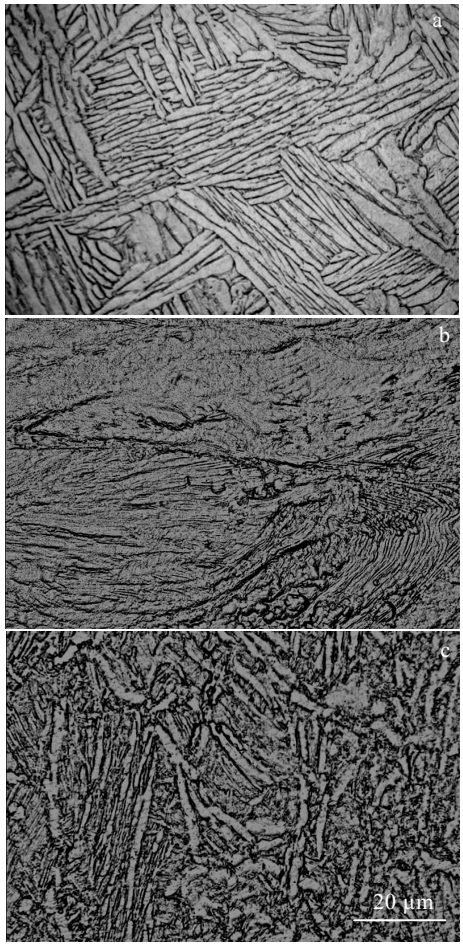

Fig.6 OM micrographs of the specimens under different thermal conditions: (a) P2, (b) P3, and (c) P4

Fig.8 shows TEM micrographs of P2, P3 and P4 specimens. Parallel platelet α was arranged in the lamellar structure, and the width of the α lamellar structure reached approximately 300 nm for P2 specimen (Fig.8a). Subgrain of a spindle-shaped particle (700 nm×1000 nm) was observed in some area of the β-phase matrix layer after deformation (Fig.8b). The microstructure of P4 specimen showed that equiaxed grains with sizes typically in the range of 324~706 nm (Fig.8c).

2.2.3 XRD analysis

XRD patterns of specimens showed α peak being the major peak, α' and α'' peak being the minor peak (Fig. 9). The presence of α' and α'' was attributed to water quenching from elevated temperature. The appearance of (110)β peak at 75.5° verified the presence of β phase in the specimens.

2.3 Microstructural evolution under different processing conditions

The microstructure of initial material was a $\alpha+\beta$ mixture (Fig.4). It came from annealing processing. The Ti-6Al-4V alloy would have good formability due to a lower hardness

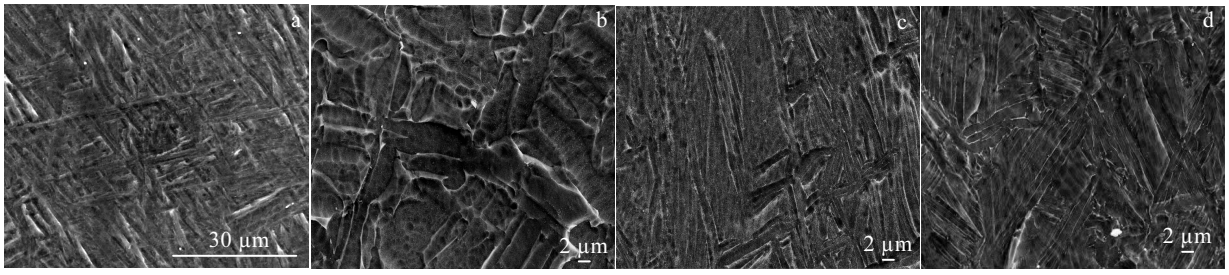

Fig.7 SEM micrographs of the specimens under different processing conditions: (a) P1, (b) P2, (c) P3, and (d) P4

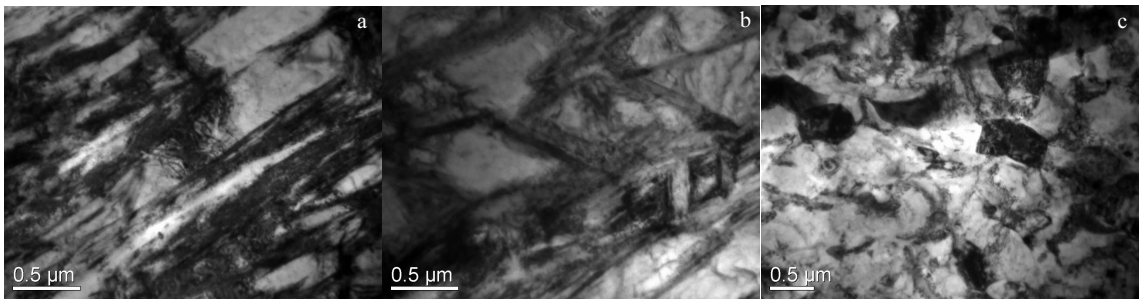

Fig.8 TEM micrographs of the specimens under different processing conditions: (a) P2, (b) P3, and (c) P4

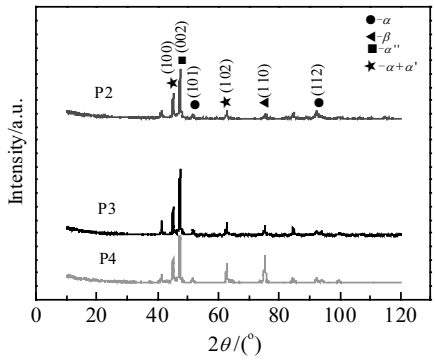

Fig.9 XRD patterns of specimens under different processing conditions

(Fig.2), and at the same, high yield and ultimate tensile strengths would be lost. The microstructural evolution under different processing conditions is schematically shown in Fig.10.

Initial microstructure was changed by TMP. The morphology of the α lamellar structure transformed to a series of coarse parallel platelet α and colonies during four kinds of processing. Fine α'-lamellae having various orientations (variants) within coarse prior β grains was obtained by solution treatment in P1 specimen, and this is 100% α' martensite microstructure (Fig. 5, 7a). The hardness of the specimen after solution treatment increased (Fig. 2), that is P1 specimen would possess higher strength and ductility comparable to the bimodal microstructures of initial material. Substantial benefits in yield, tensile and fatigue strengths can be achieved when the Ti-6Al-4V alloy is solution treated[18].

Clarifications of the phase transformations occurring during thermal processing, particularly during cooling from elevated temperature, were necessary to obtain optimal mechanical performance of α + β titanium alloys. Widmanstatten α-phase started to grow in the course of cooling and isothermal holding, which resulted in further growth of the grain boundary Widmanstatten α plates into the centre of grains (Fig. 6a, 7b). The time was enough to form a width of 300 nm of Widmanstatten α-phase immediately upon cooling in the lamellar structure (Fig. 8a). The β phase was found not only in P2 specimen, but also in all other processed specimens (Fig. 9). The appearance of even a small amount of β-phase in a Ti-6Al-4V alloy will make a contribution to superplasticity by inhibiting significant grain growth and thereby promoting grain boundary sliding[19].

Water quenching resulted in the appearance of α' and α'' phases in these specimens (Fig. 9). The microstructure consisted of intercrystalline α phase and transformed β

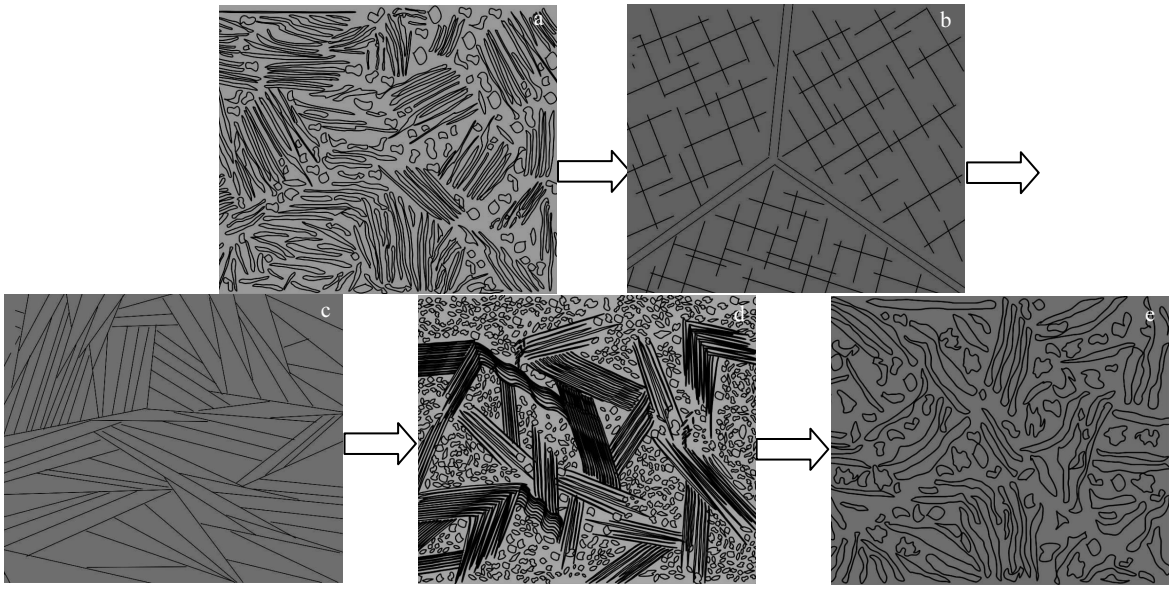

Fig.10 Schematic illustration of the microstructural evolution: (a) initial state, (b) P1, (c) P2, (d) P3, and (e) P4

phase, and orthogonal α' plates were obtained by water quenching for P1. The hardness of P2 specimen further increased (Fig.2). This means that it is possible to obtain excellent properties for this specimen.

The deformation at 850 °C can change the morphology of α grains, and the globularization of α platelets appeared in the deformed specimen (Figs. 6b, 7c). The α lamellar structure was changed by the globularization mechanism. The break-up of the prior α lamella occurred, and the metastable Widmanstatten structure converted to a more stable, colony during the thermal simulation process[20]. The dynamic globularization mechanism involves two steps: formation of sub-boundaries across α lamellae and separation of the sub-grains[21]. Two possible processes may lead to formation of sub-boundaries[21]. It is noted that the grain refining occurred in processing of deformation at 850 °C with subsequent water cooling (P3). The deformation resulted in the fragmentation of existing crystals. The thermo-mechanical processing increased the density of intragranular defects (deformation bands and twin boundaries)[22]. The deformation bends can act as nucleation sites for new phases formation and finally refine the grains. Therefore, P3 specimen exhibited the finest morphologies in SEM micrographs (Fig.7).

Hot-deformation at 850 °C accelerated the transformation of the β-phase to the α-phase, which is attributed to an increase in the number of nucleation sites for the nucleation of the α-phase. At the same time, the morphology of the α lamellar structure was changed due to deformation. The phase transformation of β to α resulted in the formation of two different morphologies of α-phase: an equiaxed structure of α grains (globular α), which mostly formed on the initial β-grain boundaries and lathes of α (acicular α) which formed on both β-grain boundaries and within the β-grain interiors[23]. TMP controlled the morphology of α phase. Deformation increased the volume fraction of globular α grains, which formed along the initial β grain boundaries, much more than that of the acicular α[23]. An equiaxed structure of α grains and the parallel lathes were obtained in P3 specimen (Figs. 6b, 7c). Fine platelet α is attributed to water quenching after deformation. It is impossible to grow up for the α platelets in this processing period (Fig. 8b). As a result, significant grain boundaries and sub-boundaries formed. The barriers of the dislocation motion increased with interphase boundary increasing, which resulted in a resistance of plastic deformation increasing[24]. As mentioned above, α' and α'' phases were present due to water quenching in P3 specimen (Fig.9). Deformation also led to the increased accumulated energy, even though 850 °C was a relatively high temperature which could provide recovery and recrystallization of the deformed structure. As a result, the maximum hardness was obtained under this processing condition. This would produce a favorable result for the mechanical properties of Ti-6Al-4V alloy.

Quenching and isothermal holding after deformation led to an increase in the width of α phase and colony. As mentioned above, two different morphologies of α grain (colony and the α lamellar structure) were formed on the deformed specimen. Platelet α started to grow from fine to coarse, and equiaxed grains increased during cooling and isothermal holding. It is more likely that new α-plates would nucleate

on the existing α-layers and that they would grow toward the β-grain interior[23]. The size of equiaxed grains was not large, even though the amount of equiaxed grains increased (Fig. 8c). As mentioned above, flow curve of P3 specimen was flow softened by larger strains (Fig. 3). The degree of softening further increased in P4 specimen. Stress relaxation occurred in the deformed specimen during cooling and isothermal holding; on the other hand, a comparison of the microstructure of P3 and P4 specimens showed that α grains of the latter were coarse lamellar and spheroidized (Fig. 6c, 7d). This means that the grain boundaries and their strengthening effect decreased under P4 condition. Therefore, the hardness of P4 specimen decreased (Fig. 2). This microstructure would provide improved combined mechanical properties.

3 Conclusions

1) The various microstructural components were obtained through different thermal simulation processing conditions in Ti-6Al-4V alloy. A fully martensitic microstructure was obtained after solution treatment. The lamellar structure formed when the specimen was water-quenched after isothermal holding at 850 °C. Equiaxed configuration appeared after deformation at 850 °C with subsequent water cooling. The microstructure was composed of α phase, lamellar colonies α/β and equiaxed configuration when the specimen was isothermally held at 600 °C after deformation at 850 °C.

2) The lowest value of hardness was obtained for initial material due to a $\alpha+\beta$ mixture. Water-quenching after solution resulted in hardness increase, and this was attributed to the presence of α' and α''. The hardness further increased for the specimen which was water-quenched after isothermal holding at 850 °C. The maximum hardness HV (5840 MPa) was obtained when the specimen was water-quenched after deformation at 850 °C. Isothermal holding at 600 °C after deformation at 850 °C decreased the hardness.

3) The deformation at 850 °C produced a structure containing globular α grains. Significant grain boundaries and sub-boundaries formed. The maximum hardness of P3 specimen was attributed to the grain boundary strengthening. Cooling and isothermal holding after deformation resulted in an increase in the dimension of the width of α phase and equiaxed configuration, which offered a range of 324~706 nm for equiaxed grains. Thus the hardness decreased.

References

1 Sadeghpour S, Abbasi S M, Morakabati M *et al. Journal of Alloys & Compounds*[J], 2018, 746(25): 206

2 Kumar P, Ramamurty U. *Acta Materialia*[J], 2019, 169: 45

3 Kumar V A, Gupta R K, *Metallurgical and Materials Transactions A: Physical Metallurgy and Materials Science*[J], 2019, 50 (6): 2702

4 Hussein M A, Azeem M, Kumar A M *et al*. *Journal of Materials Engineering and Performance*[J], 2019, 28(3): 1337

5 Jia M T, Zhang D L, Gabbitas B *et al. Scripta Materialia*[J], 2015, 107: 10

6 Rae W. *Materials Science and Technology*[J], 2019, 35(7): 747

7 Chao Q, Hodgson P D, Beladi H. *Metallurgical and Materials Transactions A*[J], 2014, 45A: 2659

8 Charlotte D F, Martin G, Prima F *et al*. *Acta Materialia*[J], 2019, 162: 149

9 Julien R, Velay V, Vidal V *et al*. *International Journal of Mechani cal Sciences*[J], 2018, 142-143: 456

10 Gangireddy S. *Metallurgical and Materials Transactions A*[J], 2018, 49(10): 4581

11 Gupta R K, Kumar V A, Kumar P R. *Journal of Materials Engineering & Performance*[J], 2016, 25(6): 1

12 Roy S, Karanth S, Suwas S. *Metallurgical and Materials Transactions A*[J], 2013, 44A: 3322

13 Zheng Y, Liu D, Yang Y H *et al. Journal of Alloys and Compounds*[J], 2018, 735: 996

14 Prakash L D G, Honniball P, Rugg D *et al. Acta Materialia* [J], 2013, 61(9): 3200

15 Zherebtsov S V, Murzinova M A, Klimova M V *et al*. *Materials Science & Engineering A*[J], 2013, 563: 168

16 Malinov S, Sha W, McKeown J J. *Computational Materials Science*[J], 2001, 21(3): 375

17 Ding R, Guo Z X, Wilson A. *Materials Science and Engineering A*[J], 2002, 327(2): 233

18 Ahmed T, Rack H J. *Materials Science and Engineering A*[J], 1998, 243(1-2) 206

19 Sergueeva A V, Stolyarov V V, Valiev R Z *et al*. *Materials Science and Engineering A*[J], 2002, 323: 318

20 Shafaat M A, Omidvar H, Fallah B. *Materials & Design*[J], 2011, 32: 4589

21 Weiss I, Froes E H, Eylon D *et al. Metall Trans A*[J], 1986, 17A: 1935

22 Manshadi A D, Dippenaar R J. *Materials Science and Engineering A* [J], 2012, 552: 451

23 Ding R, Guo Z X, Wilson A. *Materials Science and Engineering A* [J], 2002, 327(2): 233

24 Li Z, Wu D. *Materials Science and Engineering A*[J], 2007, 452-453: 15

Ti-6Al-4V 合金在不同工艺条件下水淬后的组织演变

张润奇[1]，蔡一钦[1]，李　壮[1]，李晋宇[1]，周 琦[2]，崔席郡[1]

(1. 沈阳航空航天大学 材料科学与工程学院，辽宁 沈阳 110136)

(2. 沈阳理工大学 环境与化学工程学院，辽宁 沈阳 110159)

摘　要：为了获得 Ti-6Al-4V 合金最佳的机械性能，重点在于了解在不同工艺条件下水淬后的微观结构演变。可使用热模拟机进行 Ti-6Al-4V 合金的热模拟。结果表明，试样经过固溶处理后可获得完全的马氏体组织。固溶后水淬导致硬度增加，这归因于 α'和 α''的存在。试样在 850 ℃等温保温且进行水淬后形成层状结构，硬度进一步提高。850 ℃下经变形后水淬出现等轴晶，由于晶界的强化，维氏硬度(HV)达到最大值（5840 MPa）。试样在 850 ℃变形后等温保持在 600 ℃时，组织由 α 相，层状 α/β 和等轴晶粒组成。变形后的冷却及等温保温处理导致 α 相及晶粒尺寸增大，其尺寸范围在 324~706 nm 之间，导致硬度降低。

关键词：Ti-6Al-4V合金；水淬；等温保温；层状结构；硬度

作者简介：张润奇，男，1996 年生，硕士，沈阳航空航天大学材料科学与工程学院，辽宁 沈阳 110136，电话：024-31523380，E-mail: 1293161512@qq.com